B4.0 LAKE A17 (WHALE TAIL LAKE)

Figure B-13: Shallow shoreline with gravel and cobble beach inserted with large boulders (looking northeast)

Figure B-14: Shallow shoreline with gravel and cobble beach inserted with large boulders (looking south)

Figure B-15: Lake A17 (Whale Tail Lake) outlet channel looking upstream

Figure B-16: Lake A17 (Whale Tail Lake) outlet channel aerial view looking upstream

B5.0 LAKE A18

Figure B-17: Lake A18 outlet channel with a boulder garden, looking downstream

Figure B-18: Lake A18 outlet channel with a boulder garden, looking upstream

Figure B-19: Shoreline with boulder materials partially covered by soils and organics (looking north)

Figure B-20: Lake A18 left bank floodplain (looking south)

B6.0 LAKE A45

Figure B-21: Lake A45 outlet channel looking upstream from the left bank

Figure B-22: Shoreline with large boulders relatively shallow (looking south)

Figure B-23: Shoreline with boulder garden at the lake outlet (looking north)

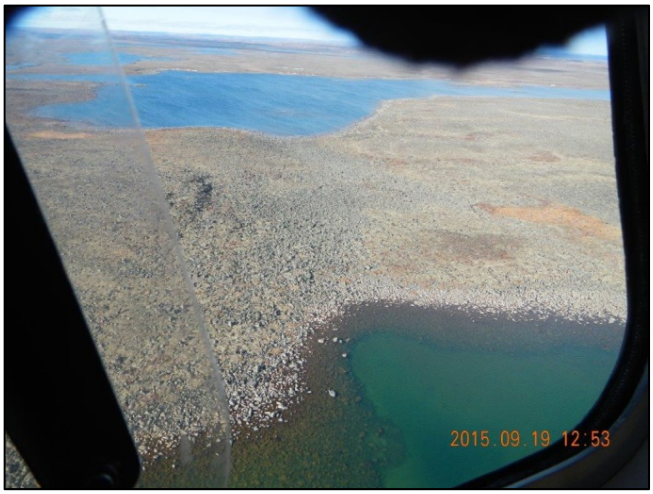

Figure B-24: Aerial view of Lake A45 outlet channel looking downstream. Undefined channel with boulder garden (looking north)

B7.0 LAKE A72

Figure B-25: Lake A72 Outlet channel, right bank looking upstream

Figure B-26: Lake A72 Outlet channel, left bank looking upstream

Figure B-27: Lake A72 Outlet channel view towards left bank at the cross section location

Figure B-28: Lake A72 Outlet channel view downstream

B8.0 LAKE A69

Figure B-29: Shoreline with large boulders (looking north)

Figure B-30: Shoreline with boulders in the shallow area (looking southeast)

Figure B-31: Shallow shoreline with larger boulders (looking west)

Figure B-32: Lakebed shoreline with gravel and cobble at the lake outlet

B9.0 LAKE A76

Figure B-33:Shoreline with large boulders and bedrock outcrop above the high water mark (looking northwest)

Figure B-34: Shoreline with boulder gardens (looking east)

Figure B-35: Shallow shoreline with cobble and boulders covered with soils and vegetation (south shore)

Figure B-36: Lake A76 main outlet channel looking upstream. Boulder gardens with shallow areas

Figure B-37: Lake A76 main outlet channel looking downstream. Boulder gardens with shallow areas and with the majority of the flow subsurface

Figure B-38: Lake A76 secondary outlet channel looking towards the right bank. Boulder gardens with no visible flow across the entire channel

APPENDIX C

Water Balance Model

Table of Contents

TABLES

FIGURES

C1.0 INTRODUCTION

A water balance model was developed for the baseline study area (BSA) to assess mean characteristics and natural variability of discharge and water levels of lake outlets in the baseline area. This appendix describes the water balance model including input data, model structure, calibration, preliminary validation, and results.

The water balance model was developed using GoldSim software with a 1-hour time step and input data for the period of 1950 to 2015. Model output results were obtained for all years, with the exception of years with meteorological input data gaps, including years 1951, 1979, 1993, and 2010, which were not modeled. The basic water balance elements for each modeled lake reservoir considered rainfall and snowmelt runoff, lake evaporation, changes in lake storage, and outflow to downstream watersheds.

The model was calibrated using runoff coefficients for land surfaces, lake outlet stage-discharge rating curves, and degree-day models for snowmelt and formation of ice in outlet channels. Runoff coefficients for land surfaces account for water losses to storage and summer evapotranspiration. The runoff coefficients were calibrated to the calculated annual water yield of hydrometric stations with available data for most of the 2015 open water season (i.e., stations with a period of record of 97 days or greater). Lake outlet stage-discharge rating curves and degree-day models were calibrated to site-specific data.

The calibrated model was used to generate daily time series data sets of lake stages and lake outlet discharges for the BSA. Frequency analyses were completed for key sites to provide a derived historical baseline of lake stage and lake outlet discharge regimes.

C2.0 MODEL STRUCTURE

Each lake in the BSA with a surface area greater than 20 hectares (ha) was modeled as a reservoir as described in the schematic diagrams (Figure C-1; Figure C-2). Inflows to the reservoir consisted of inflows from upstream watersheds and local watershed rainfall and snowmelt, including a runoff coefficient to account for storage and evapotranspiration losses. Snow-water equivalents (SWE) were calculated based on a sublimation adjustment to account for snowpack losses, and snowmelt rates were calculated using a degree-day model. Outflows consisted of lake outlet discharges and evaporative losses. Modeled lakes accounted for differences between inputs and outputs by calculating corresponding changes in lake stages and storage volumes.

A key assumption of the model is that losses to deep groundwater and changes to shallow groundwater storage are not significant due to the local permafrost regime and the associated low connectivity of shallow and deep groundwater systems.

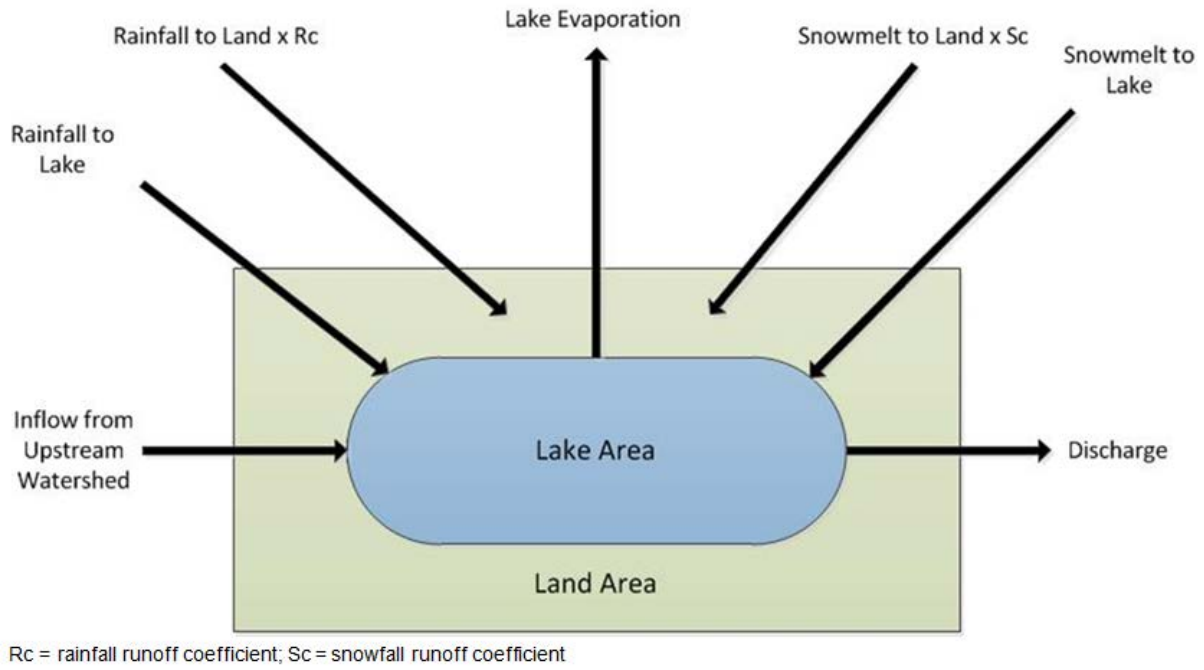

Figure C-1: Schematic of Typical Lake Reservoir Model

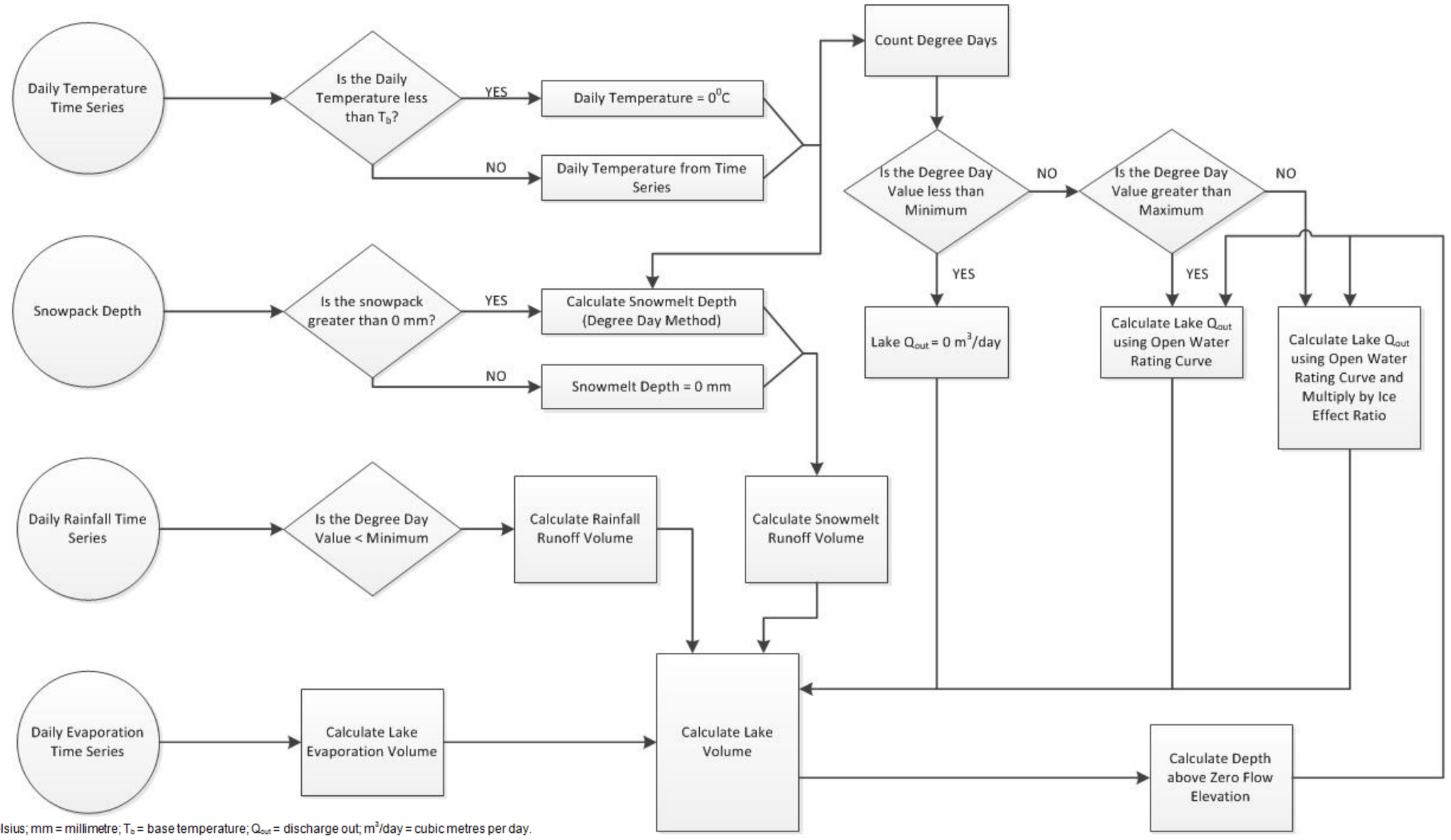

°C = degrees Celsius; mm = millimetre; T_b = base temperature; Q_{out} = discharge out; m^3/day = cubic metres per day.

Figure C-2: Water Balance Model Flowchart

C2.1 Meteorological Data

Meteorological data were available from the Baker Lake A meteorological station (Station ID 2300500) operated by the Government of Canada (2015) from 1946 to 2015, and from the Meadowbank Gold Mine (Meadowbank) from 1997 to 2003 (AMEC 2003) and from 2013 to 2015 (provided by Agnico Eagle).

Meteorological data were based on the following datasets:

- Temperature and precipitation from 1950 to 2013 were based on mean daily data available from Baker Lake A. Years with large data gaps (for the purpose of this model, defined as 20 or more days of missing data), including years 1946 to 1949, 1951, 1979, 1993, and 2010, were not considered in the model.

  Temperature was based on mean daily temperature, spatially adjusted using the following equation (AMEC 2003):

  *Mean Daily Temperature (Local) = 1.01 * Mean Daily Temperature (Baker Lake) – 0.63*

  Precipitation was based on mean daily rainfall and mean daily (SWE) derived from the difference between daily precipitation and mean daily rainfall. Precipitation was adjusted for undercatch as follows (AMEC 2003):

  *Adjusted Rainfall = Rainfall * 1.15*

  *Adjusted Snowfall = Snowfall * 1.55*

  *Adjusted Precipitation = Precipitation * 1.38*

  Temperature and rainfall data were only partially available from 1997 to 2003 at Meadowbank (AMEC 2003), and were not considered in the model.

- Temperature and precipitation from 2014 to 2015 were based on mean daily data available from Meadowbank. While data were also available for Year 2013, Year 2013 contains large data gaps (with 159 days missing) and was not considered in the model. Temperature was based on mean daily temperature data. Precipitation is collected by a rain gauge and a canister. Snowfall collected in the canister is melted at room temperature and poured into the rain gauge, and both rainfall and snowfall are recorded as precipitation. As such, the precipitation record was split between rainfall and SWE based on concurrent mean daily temperature data. Rainfall was assumed when mean daily temperatures were greater than 0ºC, and SWE was assumed when mean daily temperatures were equal to or less than 0ºC. Recorded trace events were assigned a value of 0 millimetres (mm) of precipitation. The precipitation record includes “large” (i.e., defined, for the purpose of this section, as exceeding 10 days per month) data gaps in November 2014 (13 days missing), January (16 days missing) and June (14 days missing) 2015. Gaps were assigned a value of 0 mm. Precipitation was adjusted for undercatch using the adjustment factors presented above.

- Evaporation was based on mean monthly evaporation derived from previous baseline studies (AMEC 2003), and was applied as a constant daily value for each month.

C2.2 Watershed Characteristics

Watershed delineation and analysis were based on available DEM data (PhotoSat 2015), as discussed in Section 2.2.

C2.2.1 Land and Lake Areas

Seventy-four lakes with surface areas greater than 20 ha were modeled, including 54 lakes in the A watershed, four lakes in the B watershed, 15 lakes in the C watershed, and Lake DS1. Lake DS1 has a large and complex watershed and the lake was modeled using a lumped area for its tributaries, other than the A, B, and C watersheds, which were modeled explicitly. Local watershed, lake, tributary, and land areas are presented in Table C-1 for each modeled lake.

Table C-1: Local Watershed, Lake, Tributary, and Land Areas of Modeled Lakes (km^2)

Name	Local Watershed	Lake	Tributary	Land	Name	Local Watershed	Lake	Tributary	Land
A10	0.578	0.230	0.00921	0.339	**A63**	0.480	0.0792	0	0.401
A103	0.692	0.0583	0	0.634	**A65**	3.28	0.589	0.0378	2.65
A104	1.44	0.108	0	1.33	**A69**	7.88	0.464	0.0313	7.38
A106	0.73	0.107	0.0820	0.541	**A75**	1.81	0.180	0.000553	1.63
A108	0.854	0.221	0.0241	0.609	**A76**	2.94	0.710	0.0471	2.18
A11	4.18	0.430	0.0385	3.71	**A8**	0.896	0.118	0.000992	0.777
A12	1.58	0.289	0.0211	1.27	**A81**	6.08	1.31	0.0191	4.75
A15	2.12	0.333	0.0114	1.77	**A82**	6.02	0.292	0.109	5.62
A16	7.45	1.48	0.00904	5.96	**A83**	2.98	0.0644	0.100	2.81
A17	6.14	1.66	0.0478	4.43	**A85**	2.64	0.0589	0.0111	2.57
A18	0.985	0.158	0.0111	0.816	**A86**	0.636	0.0878	0	0.548
A19	0.609	0.0553	0.00483	0.549	**A87**	1.04	0.176	0	0.860
A20	1.72	0.530	0	1.19	**A9**	2.21	0.278	0.049	1.88
A21	1.06	0.0874	0	0.972	**A91**	0.903	0.145	0	0.758
A22	0.730	0.0496	0	0.680	**A94**	2.33	0.366	0.0512	1.92
A23	3.31	0.273	0.00292	3.03	**A95**	3.75	0.0985	0.0649	3.59
A24	2.58	0.0266	0.162	2.39	**A97**	1.60	0.144	0.0471	1.41
A25	0.322	0.0574	0.00500	0.259	**B1**	0.388	0.0128	0.0108	0.364
A26	0.342	0.109	0.000609	0.232	**B3**	2.78	0.824	0.00262	1.96
A27	1.05	0.0576	0.00700	0.980	**B5**	1.26	0.282	0.0186	0.956
A28	0.791	0.102	0	0.690	**B7**	0.382	0.0388	0	0.343
A29	0.563	0.0492	0	0.514	**C1**	1.42	0.00116	0.0578	1.37
A31	0.204	0.0269	0	0.177	**C10**	1.84	0.134	0.0202	1.68
A32	0.721	0.117	0	0.604	**C12**	0.663	0.0743	0.000831	0.588
A36	1.45	0.0429	0.0451	1.36	**C13**	0.463	0.0173	0.00597	0.440

Table C-1: Local Watershed, Lake, Tributary, and Land Areas of Modeled Lakes (km^2) (continued)

Name	Local Watershed	Lake	Tributary	Land	Name	Local Watershed	Lake	Tributary	Land
A43	0.802	0.140	0.000864	0.661	**C16**	0.198	0.0170	0.00612	0.175
A44	2.30	0.229	0.000933	2.07	**C19**	0.611	0.0389	0.0101	0.562
A45	0.535	0.0295	0	0.505	**C2**	0.738	0.0707	0.000687	0.667
A47	1.23	0.0445	0.0359	1.15	**C20**	0.230	0.0232	0.00042	0.207
A49	0.252	0.0294	0.0048	0.218	**C21**	0.240	0.0268	0.00521	0.208
A5	1.24	0.234	0	1.01	**C23**	1.42	0.438	0	0.979
A53	1.34	0.141	0.0180	1.18	**C3**	2.61	0.200	0.0392	2.37
A55	1.37	0.0764	0.0111	1.28	**C34**	0.372	0.0406	0	0.332
A56	2.79	0.228	0.0427	2.52	**C38**	3.55	1.18	0.0451	2.32
A6	0.967	0.128	0.00633	0.832	**C8**	2.81	0.610	0.127	2.07
A60	2.11	0.427	0.00396	1.68	**C9**	0.222	0.0344	0	0.187
A62	0.737	0.0597	0.000867	0.676	**DS1**	766	24.2	115	627

C2.2.2 Outlet Rating Curves

Lake outlet stage-discharge rating curves were assigned for each modeled lake using one of the following five methods, with applicability as described:

1) Stage-discharge rating curves for lake outlets with available stage-discharge relationships for most of the 2015 open water season (i.e., for a period of record of 97 days or greater) were based on site-specific stage-discharge rating curves (Section 3.2.1; Appendix A). These include the lake outlets of Lake A15, Lake A17 (Whale Tail Lake), Lake A18, Lake A69, Lake C38 (Nemo Lake), and Lake DS1.

2) The stage-discharge rating curve for Lake A5 was based on the 2015 stage-discharge rating curve for Lake A69 which is similar to the stage-discharge rating curve of Lake A5 over the monitored period.

3) Lake A12 has two outlets. In the absence of site-specific stage-discharge data, both outlets were modeled using a single rating curve based on the stage-discharge rating curve of Lake A18. The outlet discharging to Lake A11 was assigned 60% of the discharge, and the remaining portion (40%) was assigned to discharge to Lake A77. These proportions were based on instantaneous discharge measurements from August 2015 (Section 3.2.2).

4) Lake A76 has two outlets which were modeled based on field observations using two separate stage-discharge rating curves to assign most of the discharge to Lake A41, while allowing discharge to Lake A75 at high flows. In the absence of continuous site-specific stage-discharge data at both outlets, the stage-discharge rating curve of the outlet discharging to Lake A41 is based on the stage-discharge rating curve of Lake A15. The stage-discharge rating curve of the outlet discharging to Lake A75 was assumed, and was calibrated to match measured water yields at Lake A69, located downstream of Lake A76. Stage-discharge rating curves of Lake A76 are presented in Figure C-3.

5) Stage-discharge rating curves for other lakes (with the exception of upstream lakes and lakes from the C watershed) were based on the stage-discharge rating curve of the closest upstream lake with a site-specific stage-discharge rating curve (e.g., the stage-discharge rating curve of Lake A16 was based on that of Lake A17; the stage-discharge rating curve of Lake A12 was based on that of Lake A15). Stage-discharge of upstream lakes and lakes from the C watershed (other than Lake C38 [Nemo Lake]) were based on the stage-discharge rating curve of Lake A18.

The method used to develop rating curves at each modeled lake is summarized in Table C-2.

Table C-2: Outlet Stage-Discharge Rating Curves

Modeled Lake	Method Used to Develop Outlet Rating Curve
Lake A5	Lake A69
Lake A12-A11	Lake A15*0.6
Lake A12-A77	Lake A15*0.4
Lake A15	Lake A15
Lake A17 (Whale Tail Lake)	Lake A17
Lake A18	Lake A18
Lake A69	Lake A69
Lake A76-A41	Lake A15 (Figure C-3)
Lake A76-A75	Assumed (Figure C-3)
Lake C38	Lake C38
Lake DS1	Lake DS1
All other lakes	Stage-discharge rating curve from the closest upstream lake with a site-specific stage-discharge rating curve, or Lake A18 for upstream lakes and lakes from the C watershed

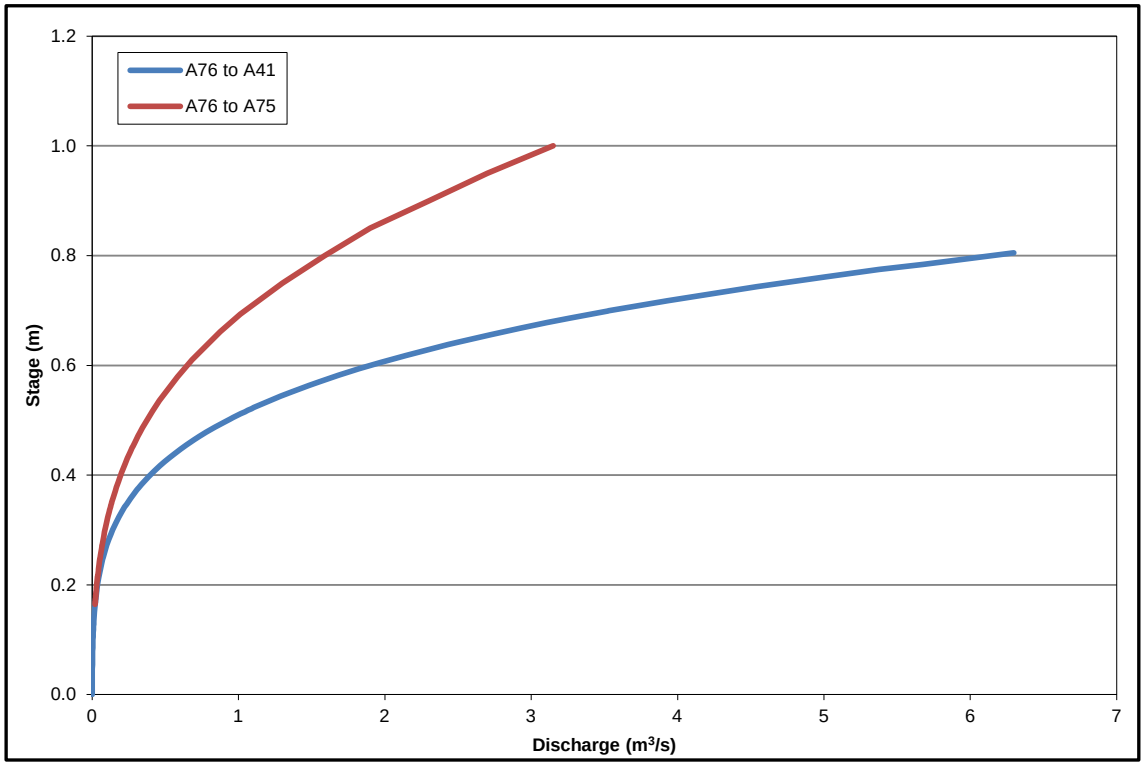

Figure C-3: Stage-Discharge Rating Curves for Lake A76

C2.3 Ice Effects on Lake Outlets

Based on field observations and general experience in the North, the opening of lake outlets during spring is generally a rapid process. This process is related to snowmelt runoff into the lake upstream of the outlet, as well as thaw of ice in the lake outlet. Flowing water provides additional thermal input, and melted or saturated snow on the outlet channel surface has a lower albedo and higher absorption of solar energy, which further accelerates melting. The change from frozen solid to fully open conditions has been observed to occur over a span of up to about four days. Lake outlets and borders are generally the first areas of open water during spring melt, while a floating ice cover may persist in the body of the lake for days or weeks after the outlet opens.

The formation of ice in winter constricts outflow channels and reduces lake discharge rates. The outlets for small lakes become constricted with ice and eventually freeze completely from approximately late October to early June each year.

A numerical relationship between lake outlet discharge and cumulative degree days was developed to account for ice effects during the freezing period in water balance modeling.

C2.3.1 Observations of Ice Formation and Degradation

Ice degradation was observed at several lake outlets during the 2015 baseline program, including outlets of Lake A15, Lake A17 (Whale Tail Lake), Lake A18, and Lake A69, as follows:

- Outlets of Lake A18 and Lake A69 were both observed to start discharging on 10 June 2015, followed by the outlet of Lake A17 on 11 June 2015, and the outlet of Lake A15 on 12 June 2015. It was noted that outlets of Lake A15 and Lake A17 may have started discharging earlier under the ice.
- The outlet of Lake A69 was free of ice on 11 June 2015. This was followed by the outlets of Lake A17 and A18 on 14 June 2015, and Lake A15 on 15 June 2015.

Ice formation was also observed by Agnico Eagle and was described in previous baseline studies (AMEC 2003) as follows:

- full ice cover was observed on small lakes on 2 October 2015;
- partial ice cover was observed on large lakes (e.g., Lake A16 [Mammoth Lake]; Lake A17 [Whale Tail]) on 2 October 2015;
- full ice cover was observed on large lakes on 12 October 2015; and
- previous baseline studies report ongoing discharge to the end of October, and to the end of November at larger lakes (AMEC 2003).

Ice formation and degradation depends on local meteorological conditions, with natural variability from year to year, but is most strongly linked to air temperature. Solar radiation also contributes to ice degradation, but historical data was not available, and air temperature may serve as a partial proxy.

C2.3.2 Method and Results

A degree-day method was developed to simulate the effect of ice conditions on discharge at each lake outlet. Degree-days were added above a base temperature of 0 degrees Celsius (°C) based on daily mean temperatures, which typically begin to exceed 0°C in early June.

The effect of ice on discharge was quantified by the following ratio:

$$\text{Ice Effect Ratio} = Q_{actual} / Q_{predicted}$$

where

Q_{actual} = Discharge measured at the outlet under ice conditions; and

$Q_{predicted}$ = Discharge predicted using an open-water rating curve for the specific outlet.

Thus, an ice effect ratio of 0 implies a frozen outlet, with no discharge, while an ice effect ratio of 1 implies an open outlet, free of ice, and fully discharging.

Ice effect ratios were developed for all modeled lakes, with the exception of Lake DS1 which was assumed to flow continuously over the winter, as follows based on observations of ice formation and ice degradation summarized in Section C2.3.1:

- For Lake A69, ice was assumed to start degrading when cumulative degree-days reach 7.8ºCd (i.e., corresponding to 10 June 2015), and the outlet was assumed to be free of ice when cumulative degree-

days reach 10.4ºCd (i.e., corresponding to 11 June 2015). This ice effect ratio is summarized in Table C-3 and shown on Figure C-4.

- For other lakes, ice was assumed to start degrading when cumulative degree-days reach 7.8ºCd (i.e., corresponding to 10 June 2015), and the outlet was assumed to be free of ice when cumulative degree-days reach 24.3ºCd (i.e., corresponding to 14 June 2015). This ice effect ratio is summarized in Table C-3 and shown on Figure C-4.
- Ice was assumed to start forming once mean daily temperatures fall below 0ºC, and outlets were assumed to be completely frozen at the end of October. As such, the ice effect ratio of 1 was assigned a negative degree day of 1ºCd, and the ice effect ratio of 0 was assigned a negative degree days of 270ºCd (corresponding to 31 October 2015), during the ice formation period. This ice effect ratio is summarized in Table C-3 and shown on Figure C-5.

Table C-3: Ice Effect Ratio Parameters

Parameter	Value
Outlet break-up – closed (Lake A69) (Ice effect ratio of 0)	7.8
Outlet break-up – open (Lake A69) (Ice effect ratio of 1)	10.4
Outlet break-up – closed (all other lakes) (Ice effect ratio of 0)	7.8
Outlet break-up – open (all other lakes) (Ice effect ratio of 1)	24.3
Outlet freeze-up – open (Ice effect ratio of 1)	1.0
Outlet freeze-up – closed (Ice effect ratio of 0)	270

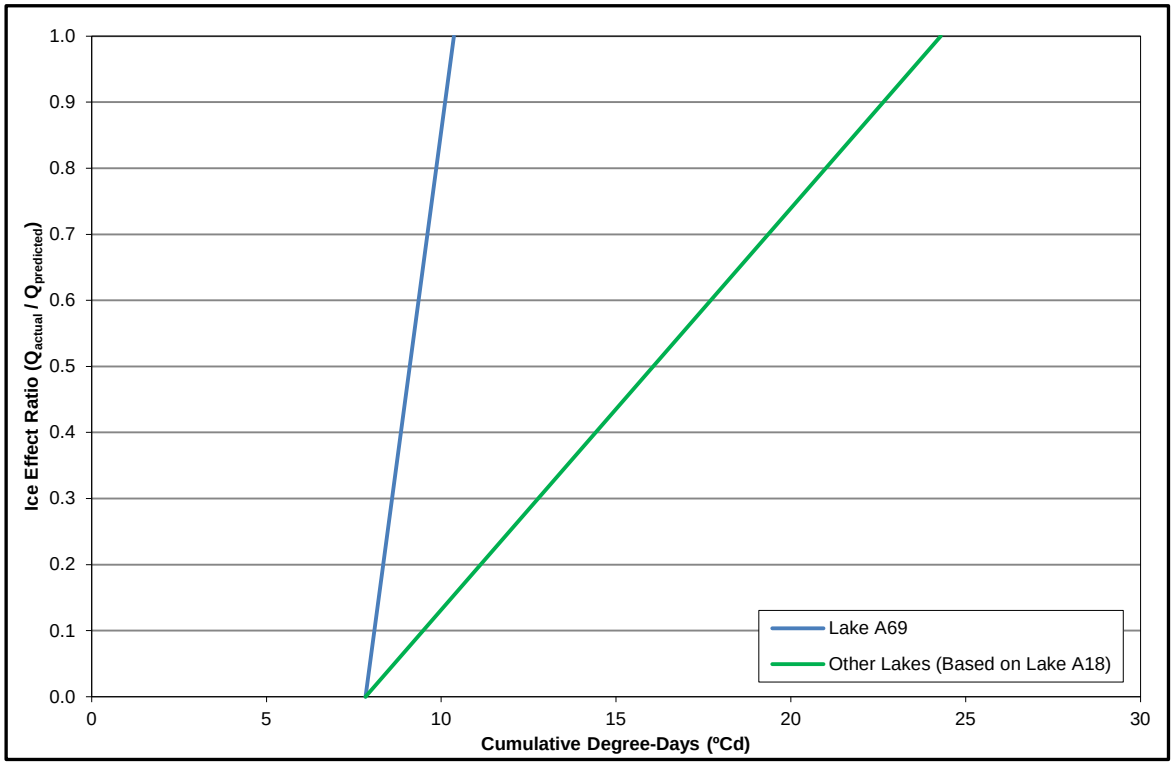

Figure C-4: Ice Degradation Period: Ice Effect Ratios and Cumulative Degree-Days

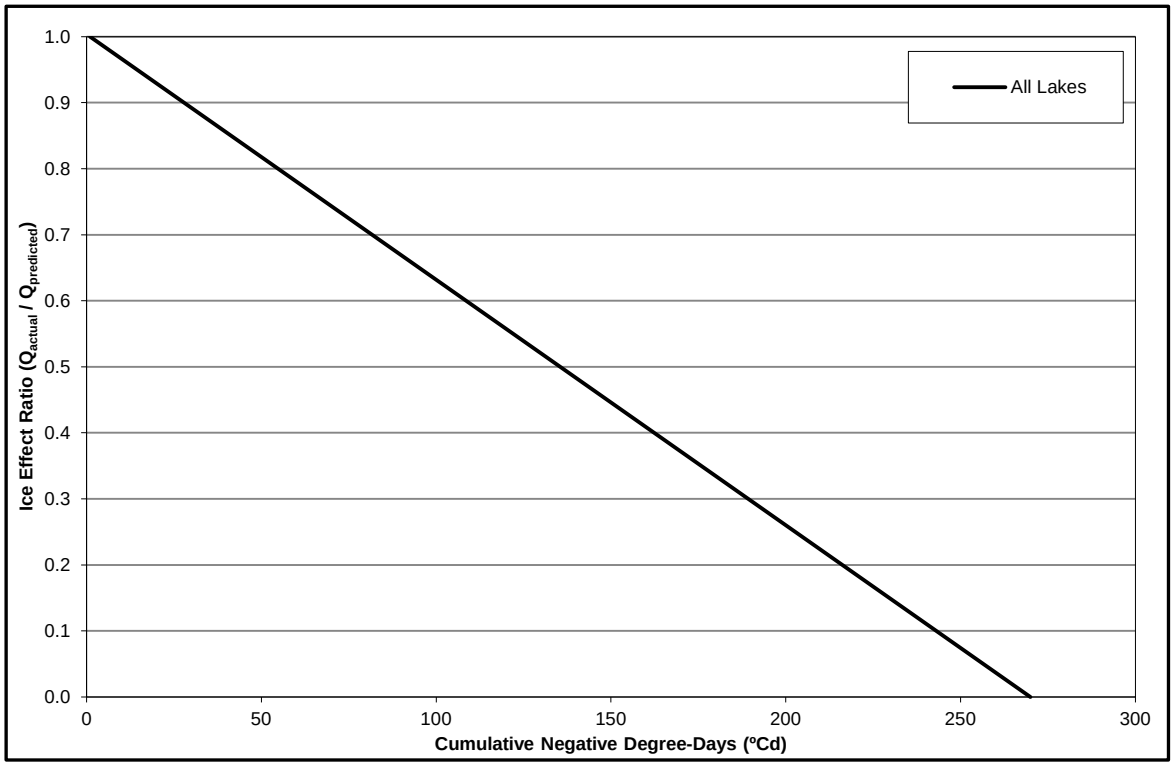

Figure C-5: Ice Formation Period: Ice Effect Ratios and Cumulative Degree-Days

C2.4 Snowmelt

Snowmelt is generated predominantly by the melting of the accumulated snowpack during the period of spring freshet. Based on experience, the spring freshet occurs over a period of several weeks and is a major contributor of overall annual precipitation and lake inflows in northern environments.

C2.4.1 Observations of Snowmelt

Snowmelt was observed during the first hydrometric field visit (from 8 to 15 June 2015). By 15 June 2015, most of the snow had melted, with any snow remaining largely located along steep slopes with lesser exposure to sunlight.

C2.4.2 Method

In the model, snowfall from the derived climate data accumulates as snowpack during fall and winter when temperatures are below freezing. A 26% reduction was applied to the modeled snowpack to represent sublimation losses based on previous baseline studies (AMEC 2003).

Snowmelt begins when the daily average temperature rises above the base temperature (T_b). The snowmelt rate is determined by Equation 1.

Equation 1: Snowmelt Equation

$$\text{Daily Snowmelt Runoff} = R_{cs} \times M_f \times (T - T_b)$$

Where

R_{cs}= Snowmelt runoff coefficient (dimensionless);

M_f = Melt factor (mm/°C);

T = Mean daily air temperature (°C); and

T_b = Base temperature (°C).

For consistency with observed snowmelt, the melt factor was set at 4.0 millimetres per degree Celsius (mm/ºC) and the base temperature at -1.0°C,. The snowmelt runoff coefficient R_{cs} was calibrated to expected freshet and annual watershed yields, and is further discussed in Section C2.5. These values resulted in a completely melted snowpack by 18 June 2015, consistent with field observations, and modeled peak discharges consistent with measured hydrographs, as shown in Section C2.5. Snowpack accumulation and melt are shown in Figure C-6 for the 2015 hydrological year (i.e., 1 October of the previous year to 30 September of the current year, as defined by previous baseline studies [AMEC 2003]).

A dispersed delay of 20 days was applied to the lumped tributaries of Lake DS1 to account for attenuations.

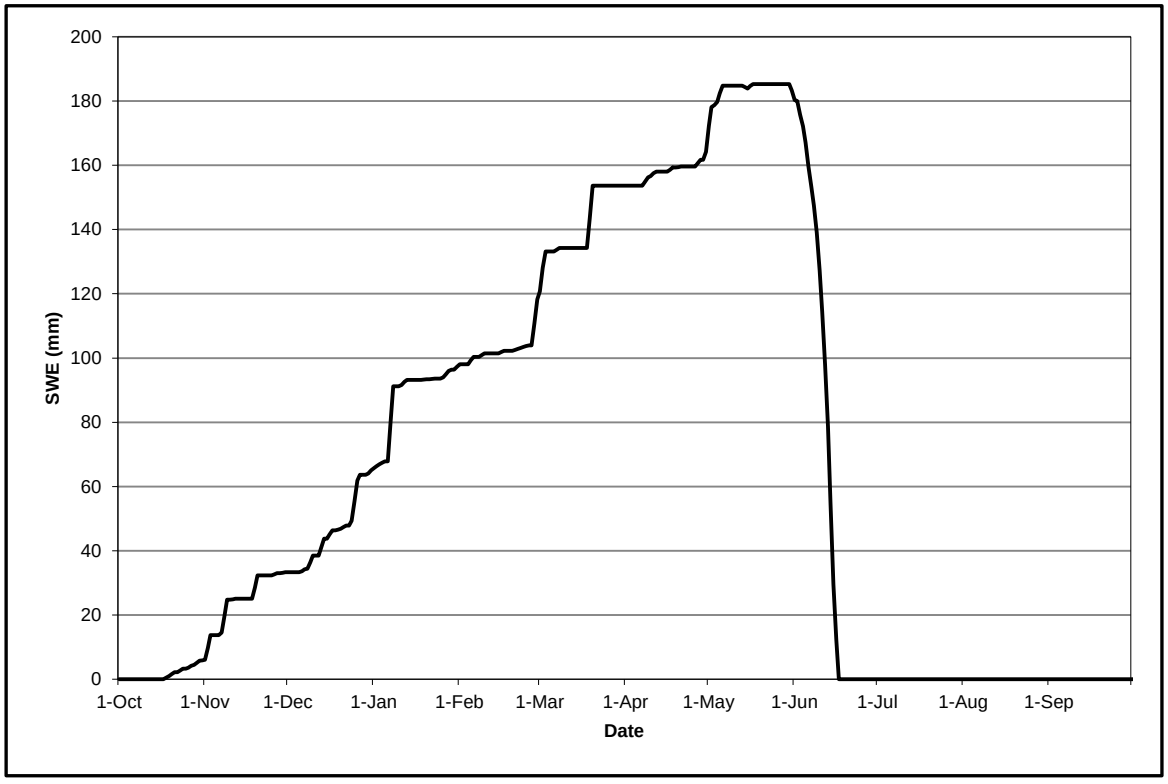

Figure C-6: 2015 Modeled Snowpack

C2.5 Model Calibration and Validation

Each modeled lake has a consistent structure and logic in the water balance. Physical characteristics of each modeled lake include local contributing lake and land areas, total discharge areas, and connectivity with other lakes.

The volume and timing of lake discharges are the predominant model outputs. The key calibration variables for the volume of water discharged are runoff coefficients, including rainfall and snowmelt runoff coefficients:

- Rainfall runoff coefficients were applied to rainfall runoff, separated by runoff on land and runoff on lake areas (i.e., direct runoff) to account for evapotranspiration and storage losses. Direct runoff coefficients were assigned a value of 1.0.
- Snowmelt runoff coefficients were applied to snowmelt runoff, separated by runoff on land and runoff on lake areas (i.e., direct runoff) to account for storage losses. Snowmelt runoff coefficients were considered separately from sublimation losses. Direct runoff coefficients were assigned a value of 1.0.

C2.5.1 Method

Rainfall and snowmelt runoff coefficients for land areas were calibrated to measured hydrographs and annual water yields. The snowmelt runoff coefficient primarily affects peak discharges, and was calibrated to measured hydrographs. The rainfall runoff coefficient was adjusted to reach measured annual water yields. There were three days of rainfall prior to peak discharges, which were considered during the calibration of the rainfall runoff coefficient.

The calibration process was as follows:

- **Calibration:** The model was run on a 1-hour time-step from 1950 to 2015 (exclusive of years 1951, 1979, 1993, and 2010) using the derived climate data set as input values. Both rainfall and snowmelt runoff coefficients were initially set to 1.0 and reduced incrementally to match the measured hydrograph and annual water yields at Lake A18 (i.e., the most upstream lake with a continuous data set).

  Derived annual water yields of Lake A17 (Whale Tail Lake) and Lake C38 (Nemo Lake) (Section 3.2.1.9) were significantly lower than those derived for Lake A18, Lake A15, Lake A69, and Lake DS1, and runoff coefficients of these local watersheds and local tributaries were reduced from those applied for Lake A18. As noted in Section 3.2.1.9, this reduction may be related to a proportion of ineffective drainage area in both local watersheds. Tributaries of Lake A17 (Whale Tail Lake) and Lake C38 (Nemo Lake) were opportunistically observed to drain poorly, with ponded water, and the potential exists for shallow subsurface flow to convey water outside of the assumed watershed boundaries.

- **Validation:** Runoff coefficients applied to Lake A18 were applied to all modeled lakes (other than Lake A17 [Whale Tail Lake] and local tributaries, and Lake C38 [Nemo Lake] and tributaries), and were verified by comparing modeled hydrographs and annual water yields to measured continuous data sets.

C2.5.2 Results

Rainfall runoff coefficients were calibrated as 1.0 for lake areas, 0.35 for land areas of local watersheds of Lake A17 (Whale Tail Lake), Lake C38 (Nemo Lake), and their tributaries, and 0.70 for land areas of all other lakes. Snowmelt runoff coefficients were calibrated as 1.0 for lake areas, 0.50 for land areas of local watersheds of Lake A17 (Whale Tail Lake), Lake C38 (Nemo Lake), and their tributaries, and 1.0 for land areas of all other lakes. A snowmelt coefficient of 1.0 is consistent with frozen ground conditions and low evaporation during the melt period; however, it may indicate that additional precipitation may not have been captured by the local climate station, or that sublimation losses may be slightly overestimated. This may only be confirmed with additional monitoring data.

The calibrated runoff coefficients result in good agreement between modeled and measured discharges, water levels, and annual water yields. Uncertainties are discussed below:

- Lake A5 appears to be well estimated at low flows; however, additional field data during the high flow period are required to validate the timing and magnitude of the peaks, and improve its stage-discharge rating curve, which, is based on that of Lake A69 in the model. Thus, peak discharges generated by the model at Lake A5 are associated with a degree of uncertainty.

- The model appears to slightly overestimate lake surface elevations of Lake A15 at low flows. This may result from its stage-discharge rating curve, which was based on two discharge measurements at high and lower flows, and a discharge estimate during the low flow season in September, which was not measurable.

- Local watersheds and tributaries of Lake A17 (Whale Tail Lake), Lake C38 (Nemo Lake) and their tributaries were assumed to be poorly drained with proportions of ineffective areas, and the potential for shallow subsurface flow to convey water outside of the assumed watershed boundaries. While consistent

with opportunistic field observations, areas of potential ineffective flows could be refined with additional observations and specifically targeted with lower runoff coefficients to improve the model.

- Stage-discharge rating curves of Lake A12 and Lake A76 were based on assumptions and calibration of water yields at Lake A69. Both lakes are comprised of two lake outlets, and assumed rating curves could be improved, and further validated, with additional field measurements.
- Recession discharges and water levels at Lake A69 are associated with a degree of uncertainty related to the timing of snowmelt runoff of upstream lakes. Thus, the recession period may be improved with additional field data at upstream lakes. Peak and low flows appear to be well matched.
- Lake DS1 was modeled coarsely with lumped tributary areas (other than the A, B, and C watersheds, which were modelled explicitly) based on physical parameters derived from available desktop data. Due its large watershed, Lake DS1 hydrology is complex and cannot accurately be reproduced by this baseline model; however the model results are considered fit for the purpose of this baseline study. Annual water yields are reasonably matched which further validate calibrated parameters. Finer scale parameters such as the timing of peaks and response to rainfall events may not be accurately estimated and should be used with caution.

Resulting runoff coefficients are presented in Table C-4.

Measured discharge data are plotted along with model output for qualitative comparison in Figure C-7 (Lake A5), Figure C-9 (Lake A15), Figure C-11 (Lake A17 [Whale Tail Lake]), Figure C-13 (Lake A18), Figure C-15 (Lake A69), Figure C-17 (Lake C8), Figure C-19 (Lake C38 [Nemo Lake]), and Figure C-21 (Lake DS1).

Comparisons of measured and modeled lake water surface elevations are presented in Figure C-8 (Lake A5), Figure C-10 (Lake A15), Figure C-12 (Lake A17 [Whale Tail Lake]), Figure C-14 (Lake A18), Figure C-16 (Lake A69), Figure C-18 (Lake C8), Figure C-20 (Lake C38 [Nemo Lake]), and Figure C-22 (Lake DS1) over the discharge period.

Comparisons of measured and modeled annual water yields are presented in Figure C-23.

Table C-4: Calibrated Runoff Coefficients

Lake	Rainfall Runoff Coefficient		Snowfall Runoff Coefficient	
	Land	Lake (Direct)	Land	Lake (Direct)
Lake A17 (Whale Tail Lake), Lake C38 (Nemo Lake)	0.35	1.0	0.50	1.0
All other lakes	0.70	1.0	1.0	1.0

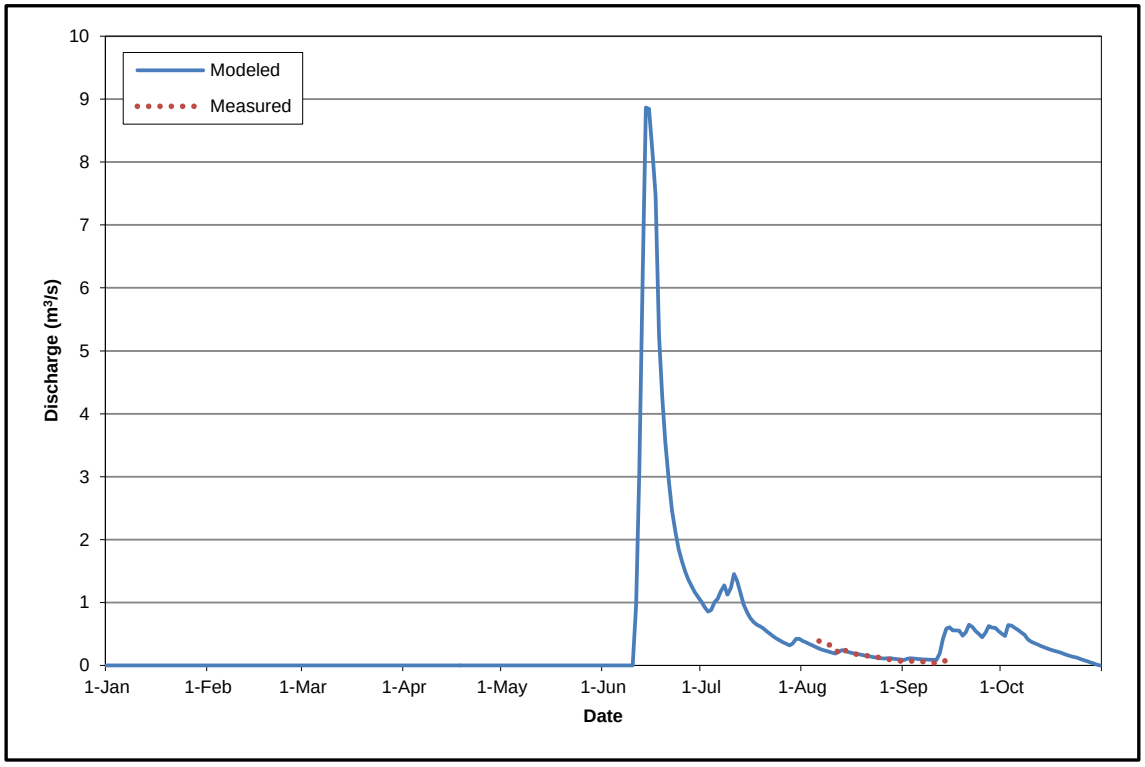

Figure C-7: Comparison of Modeled and Measured Discharge at Lake A5 in 2015

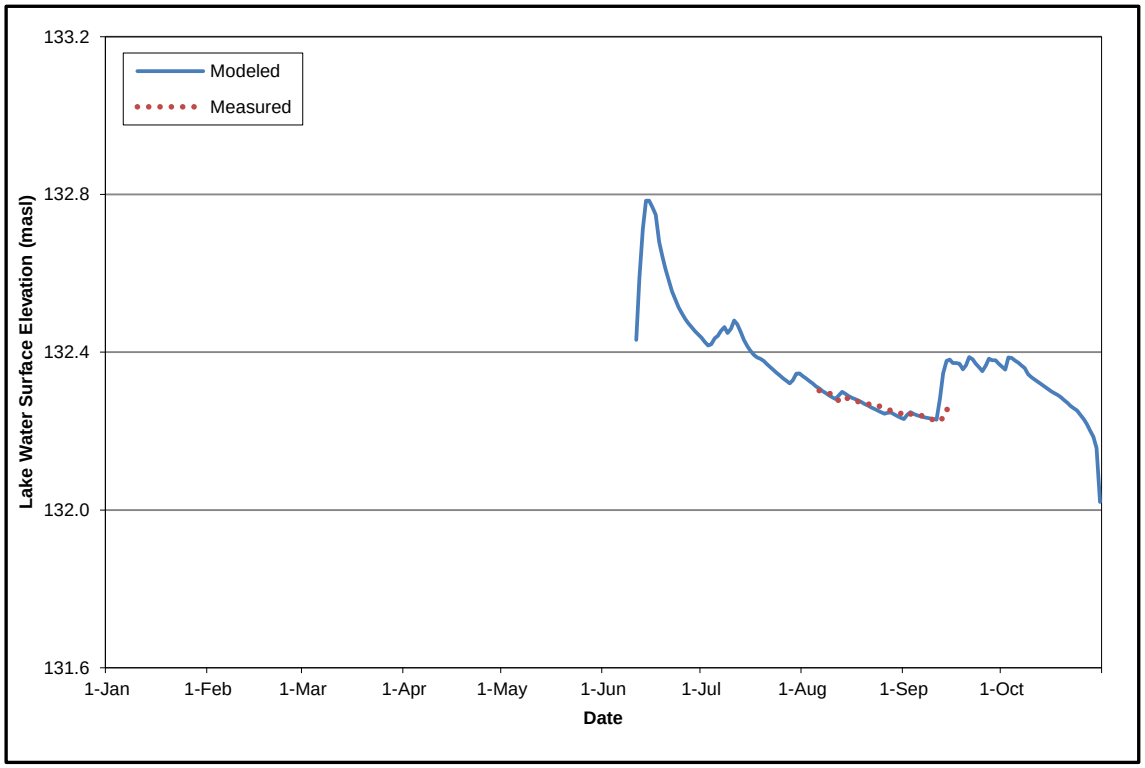

Figure C-8: Comparison of Modeled and Measured Lake Water Surface Elevation at Lake A5 in 2015

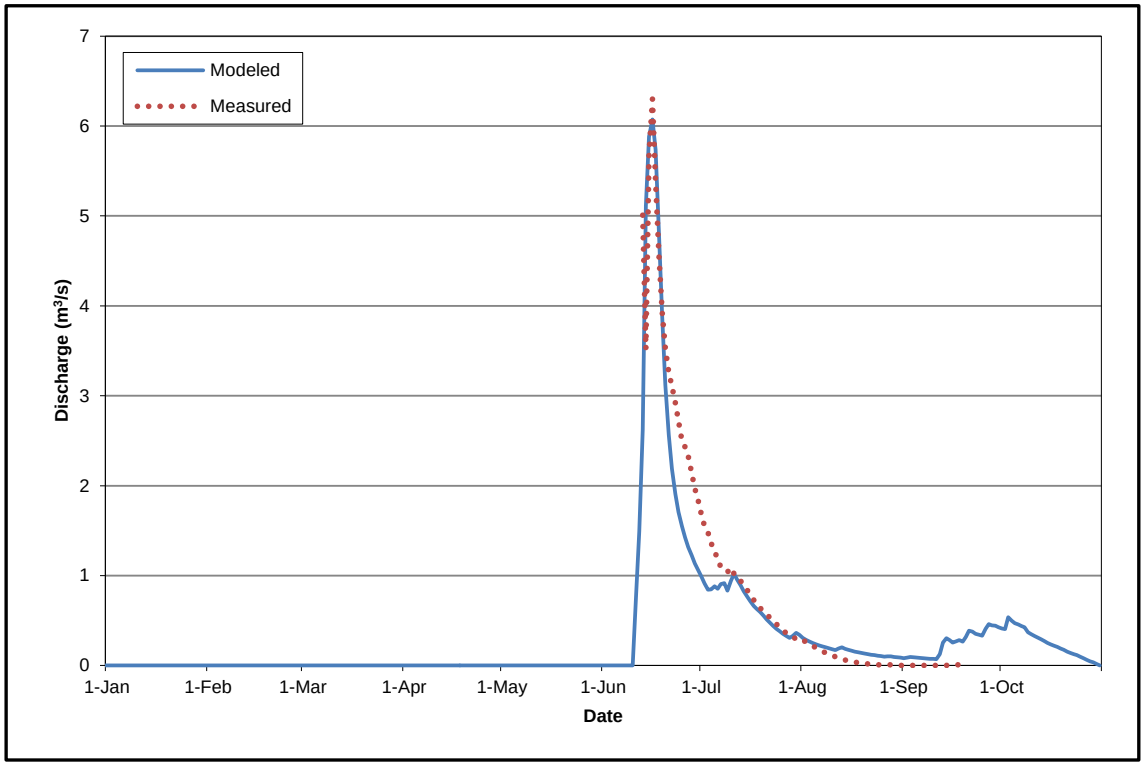

Figure C-9: Comparison of Modeled and Measured Discharge at Lake A15 in 2015

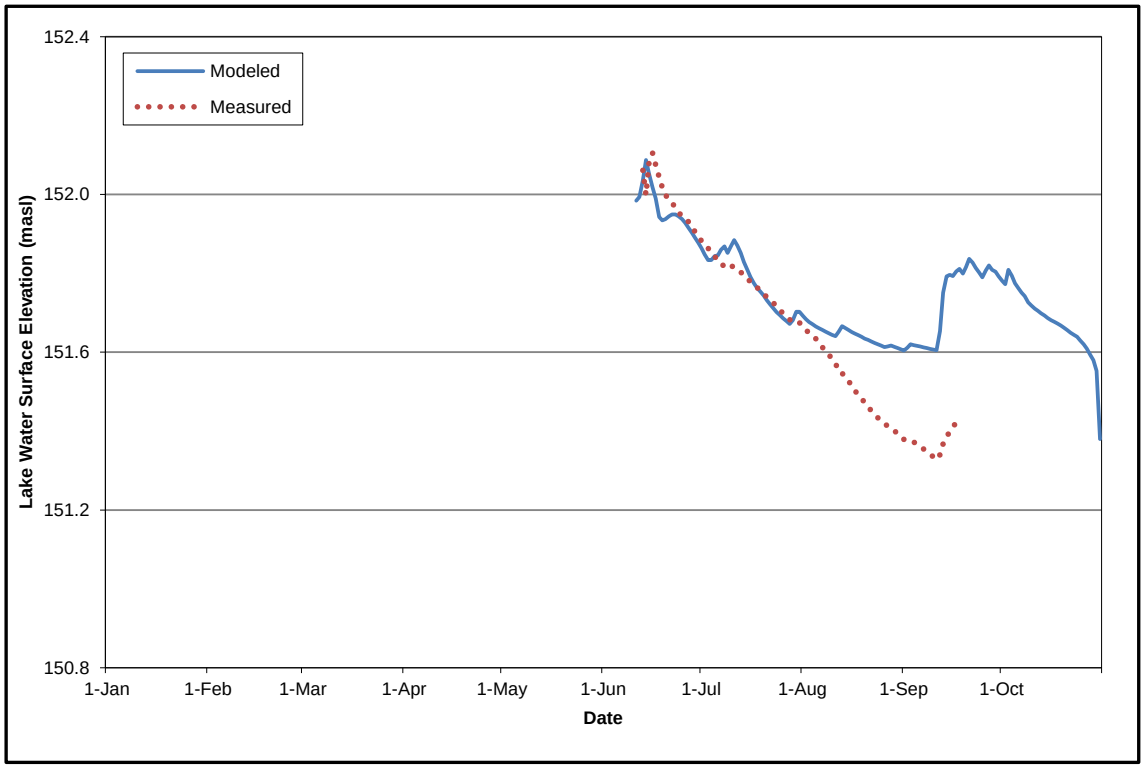

Figure C-10: Comparison of Modeled and Measured Lake Water Surface Elevation at Lake A15 in 2015

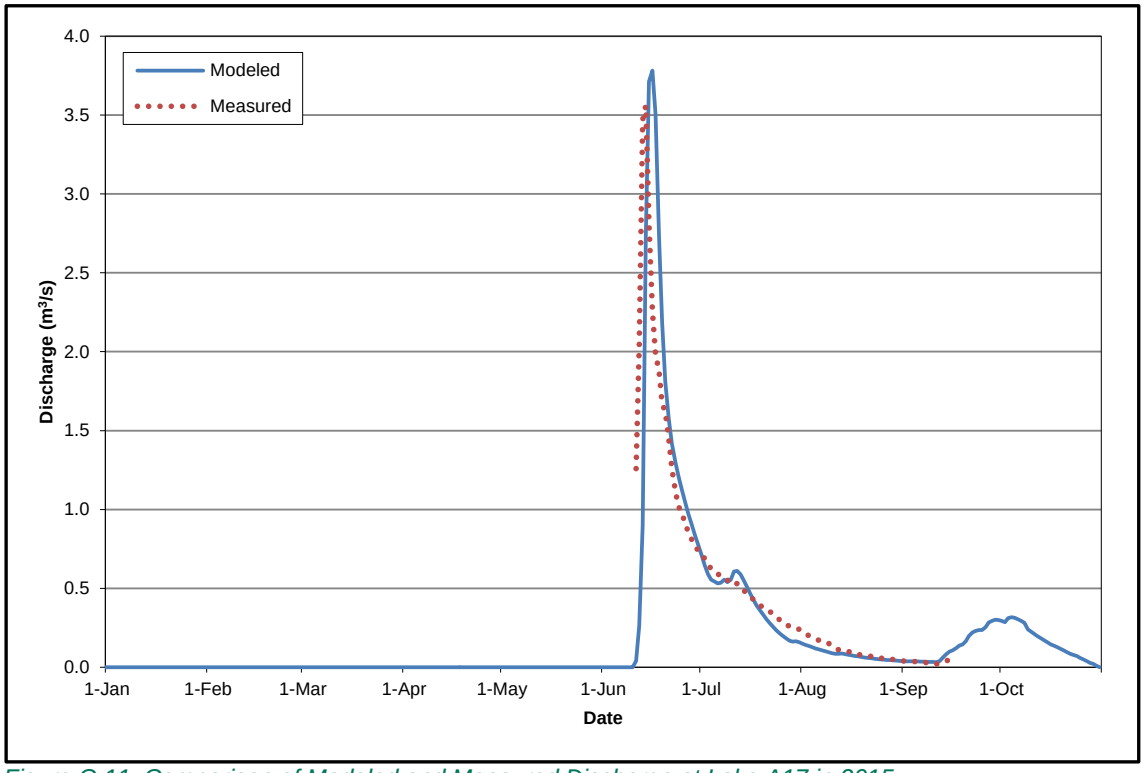

Figure C-11: Comparison of Modeled and Measured Discharge at Lake A17 in 2015

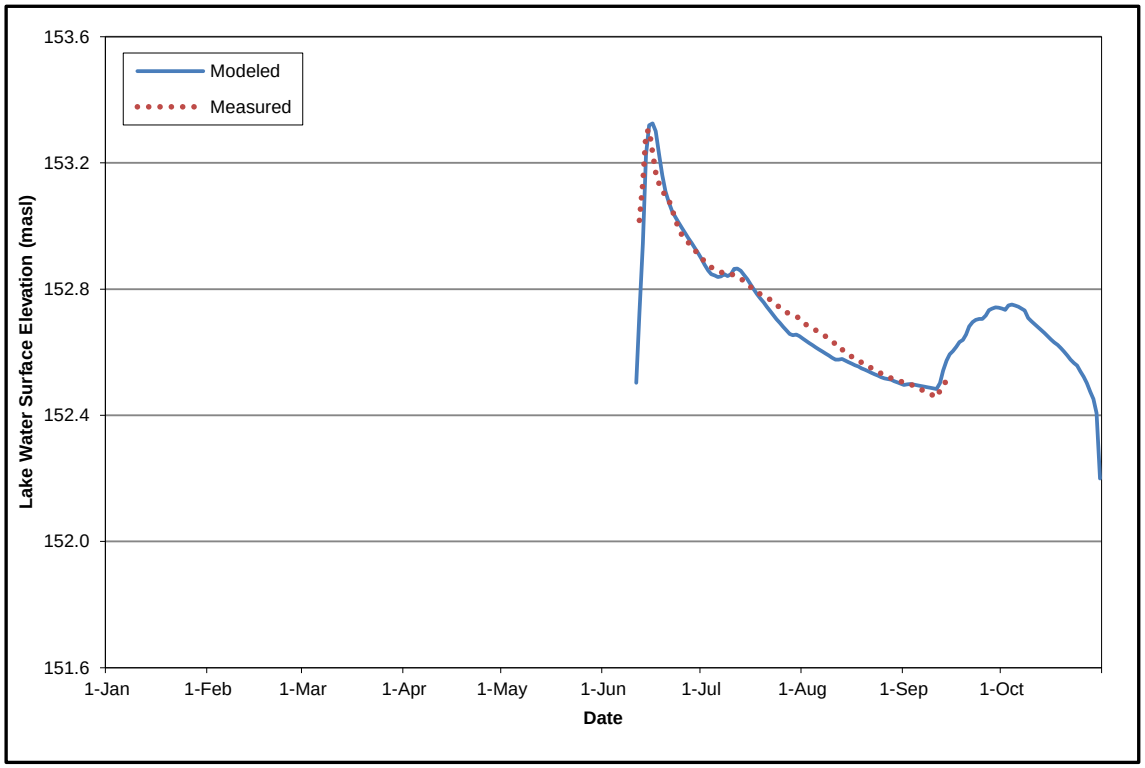

Figure C-12: Comparison of Modeled and Measured Lake Water Surface Elevation at Lake A17 in 2015

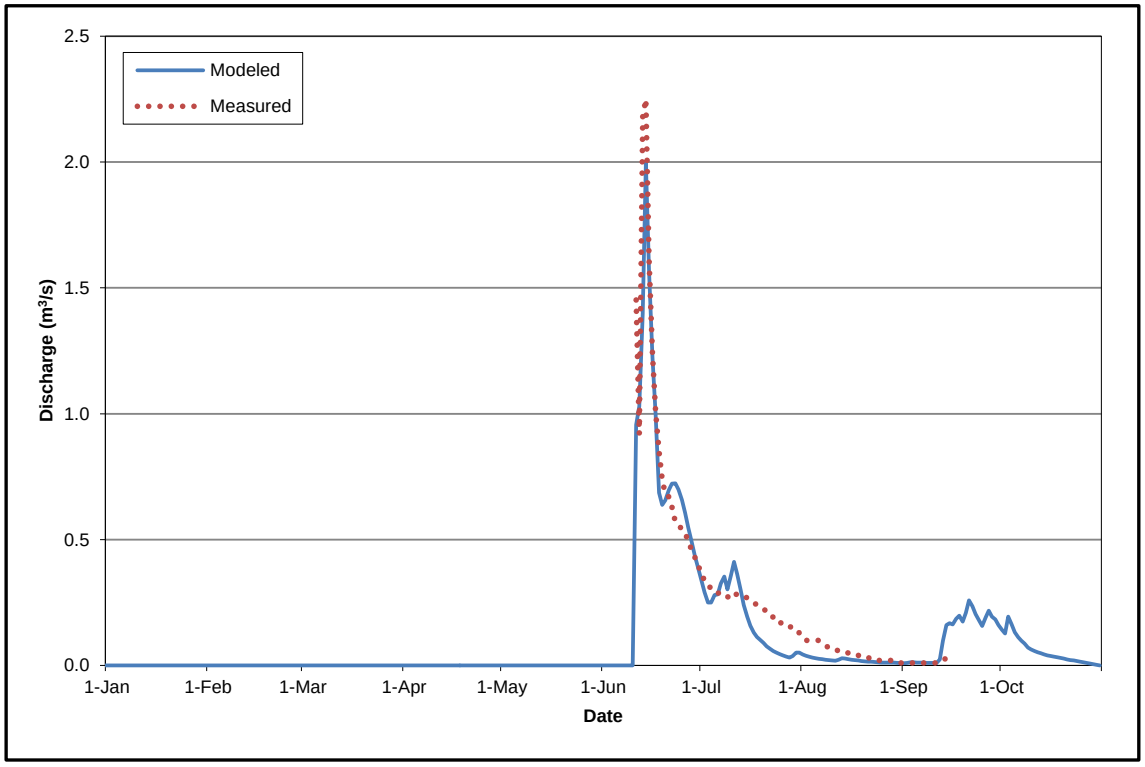

Figure C-13: Comparison of Modeled and Measured Discharge at Lake A18 in 2015

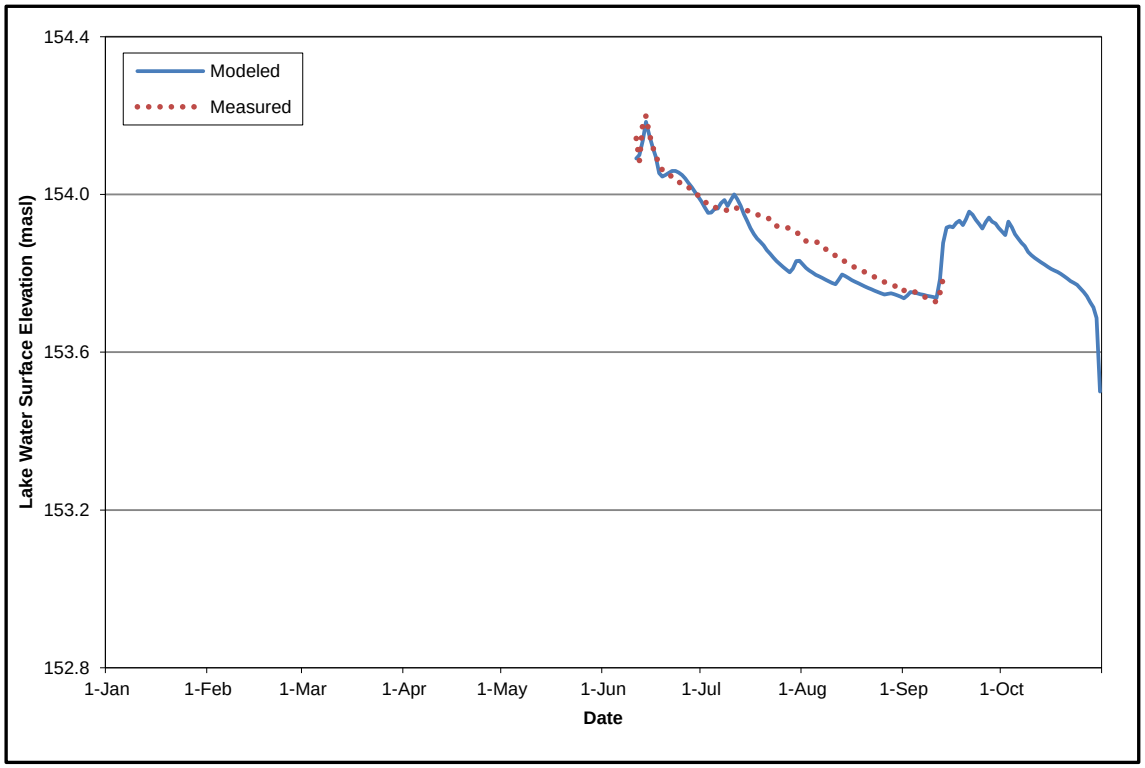

Figure C-14: Comparison of Modeled and Measured Lake Water Surface Elevation at Lake A18 in 2015

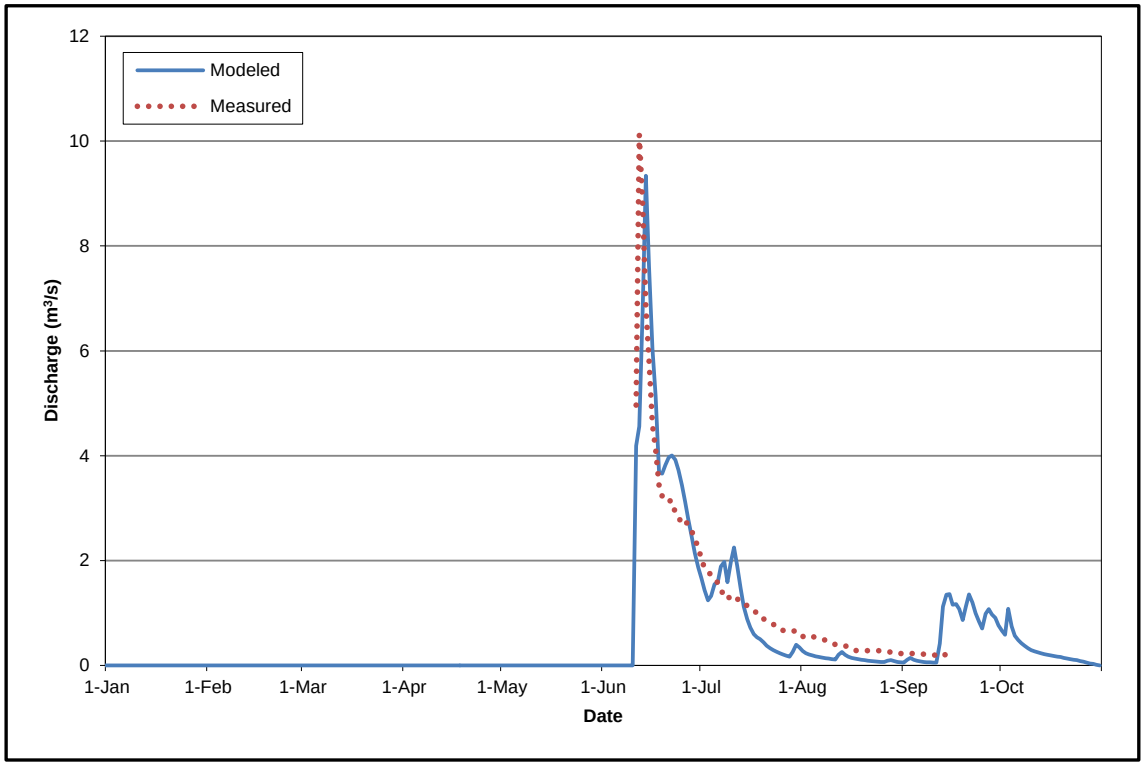

Figure C-15: Comparison of Modeled and Measured Discharge at Lake A69 in 2015

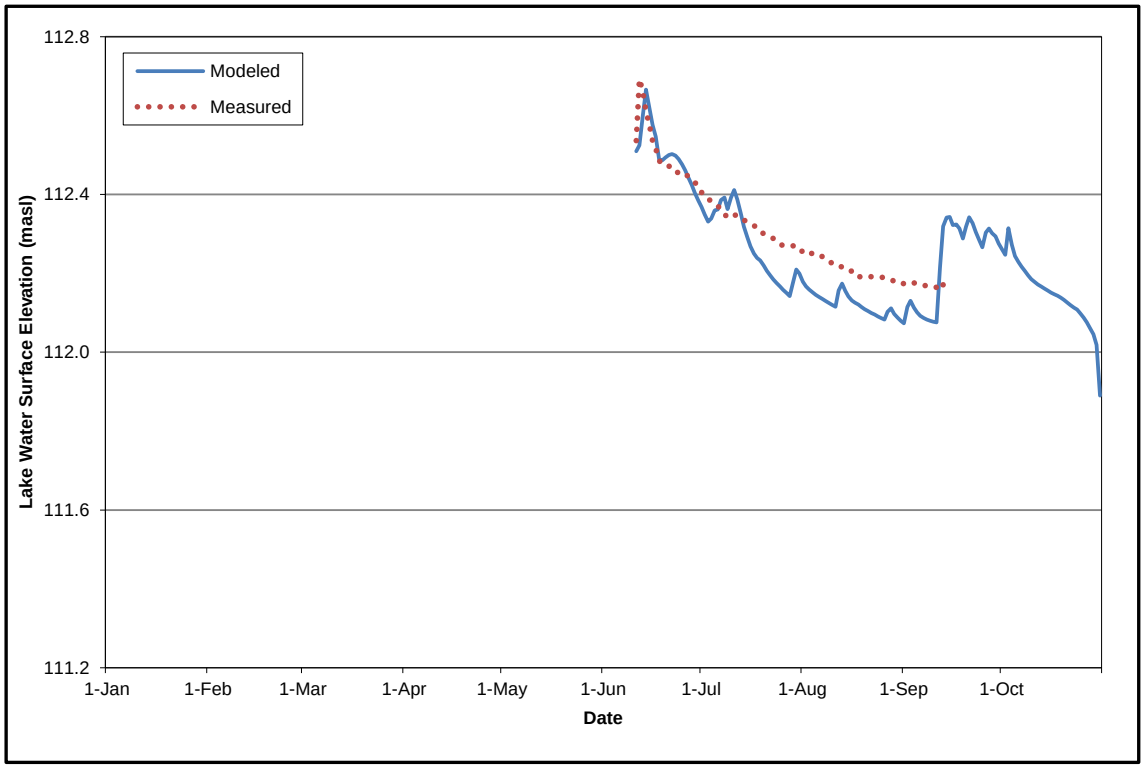

Figure C-16: Comparison of Modeled and Measured Lake Water Surface Elevation at Lake A69 in 2015

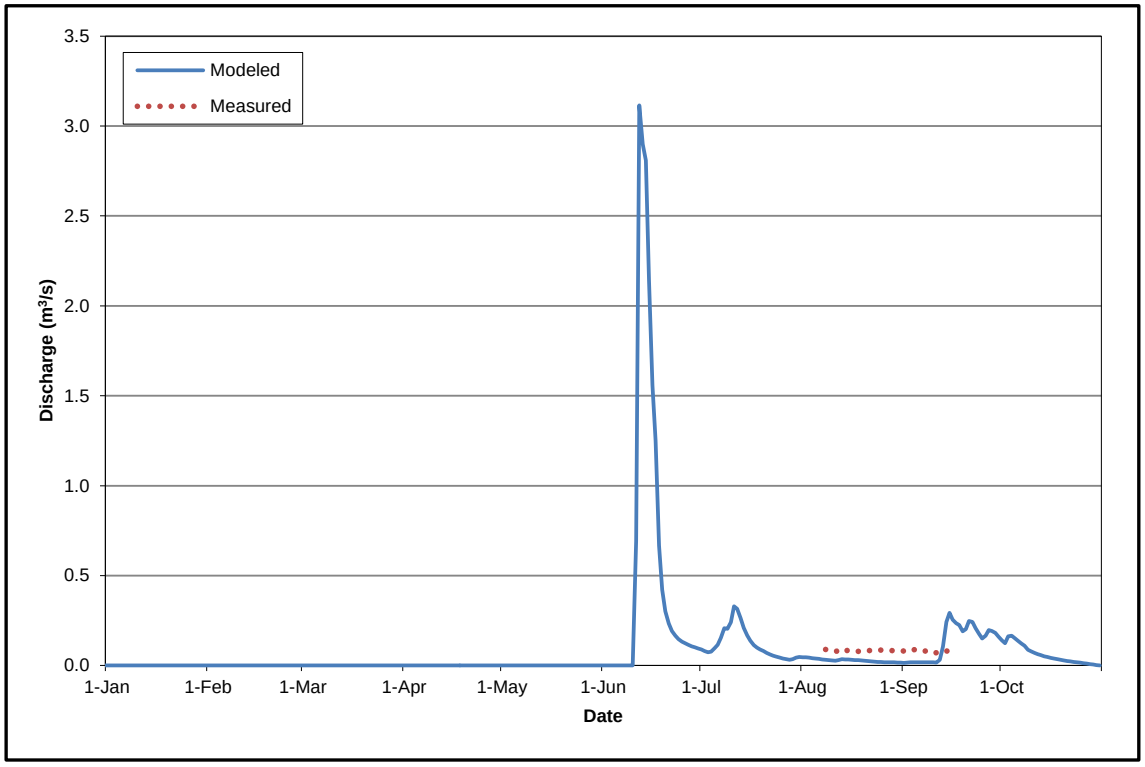

Figure C-17: Comparison of Modeled and Measured Discharge at Lake C8 in 2015

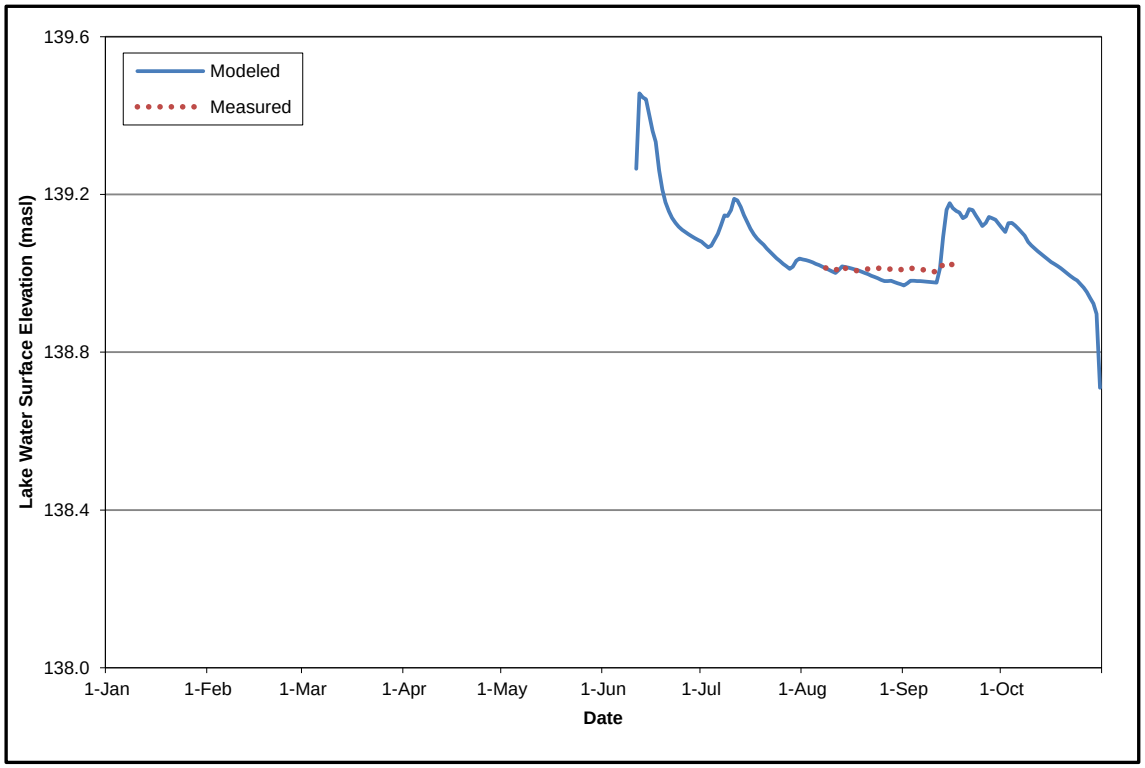

Figure C-18: Comparison of Modeled and Measured Lake Water Surface Elevation at Lake C8 in 2015

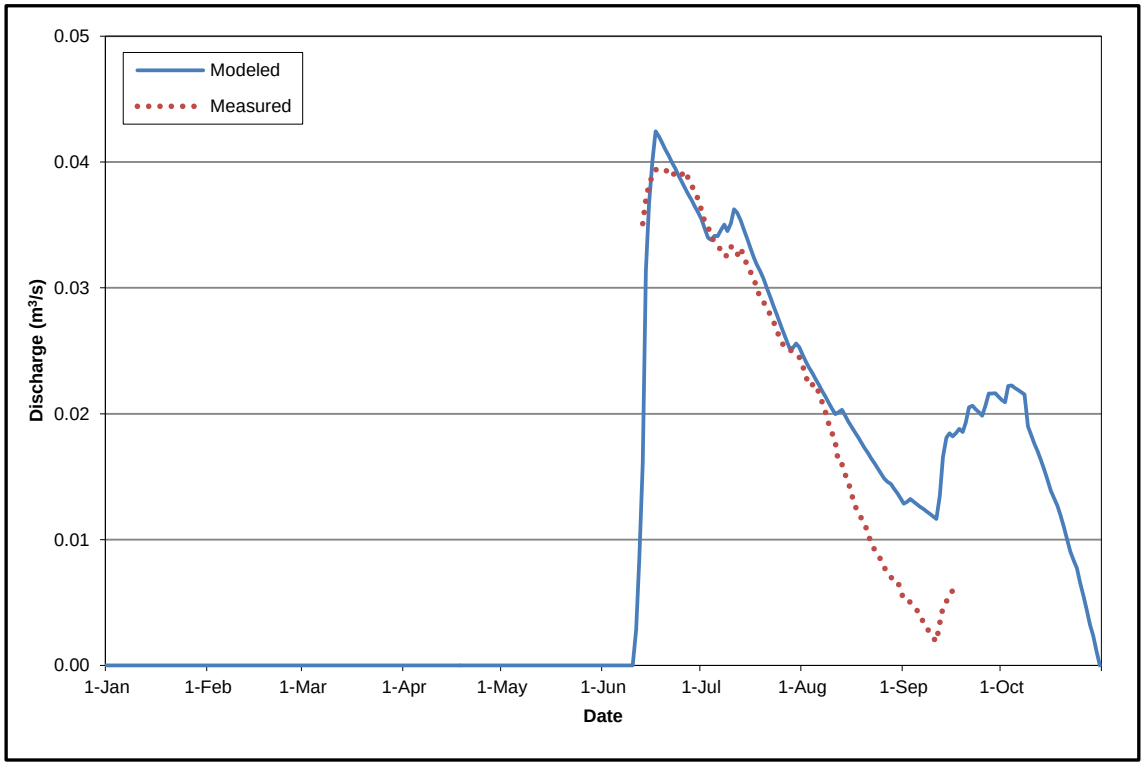

Figure C-19: Comparison of Modeled and Measured Discharge at Lake C38 in 2015

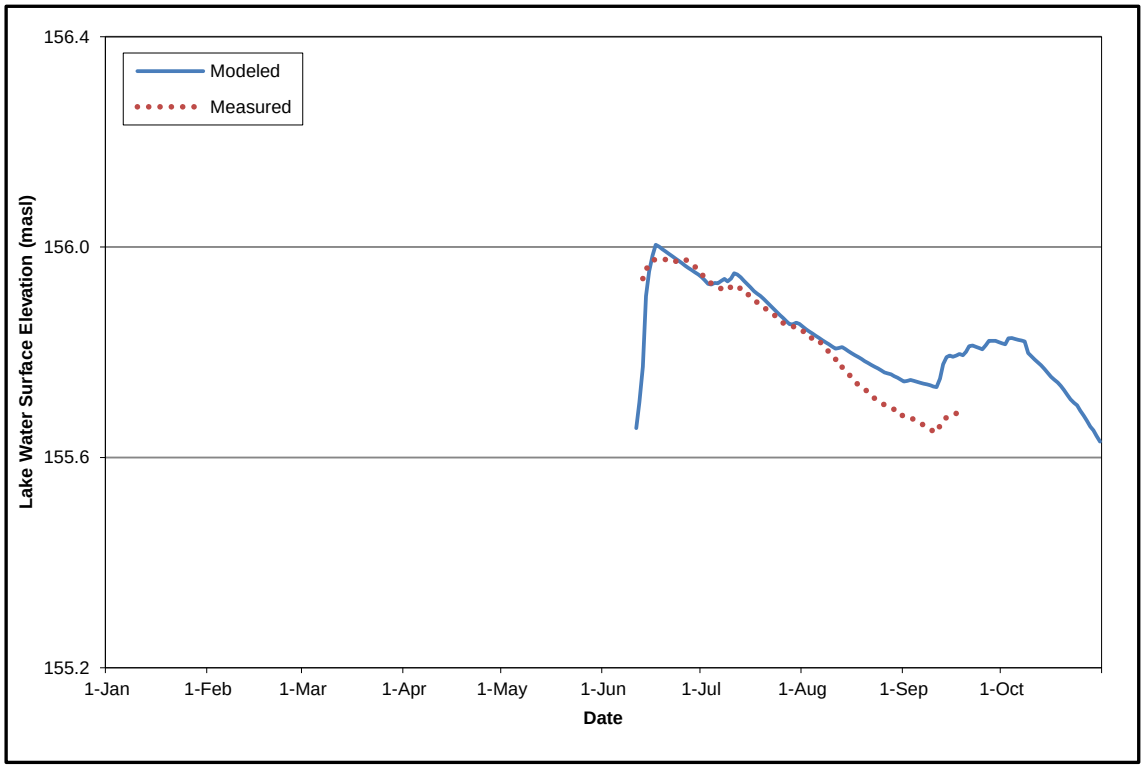

Figure C-20: Comparison of Modeled and Measured Lake Water Surface Elevation at Lake C38 in 2015

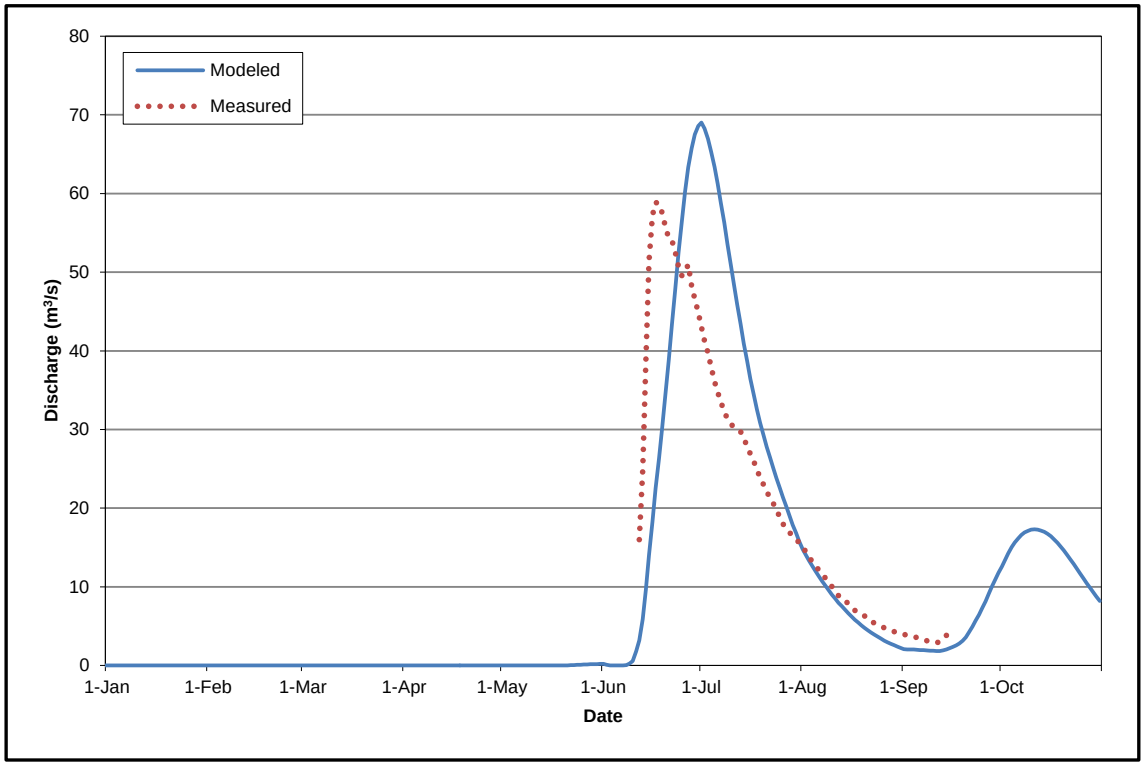

Figure C-21: Comparison of Modeled and Measured Discharge at Lake DS1 in 2015

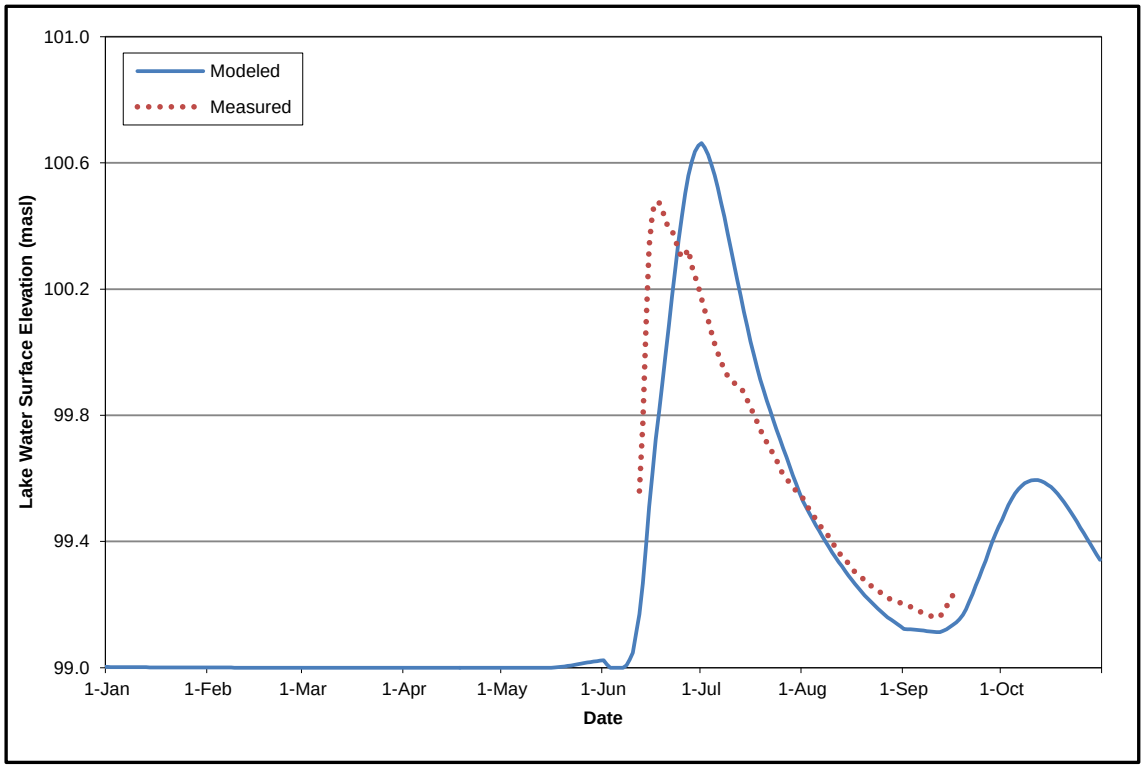

Figure C-22: Comparison of Modeled and Measured Lake Water Surface Elevation at Lake DS1 in 2015

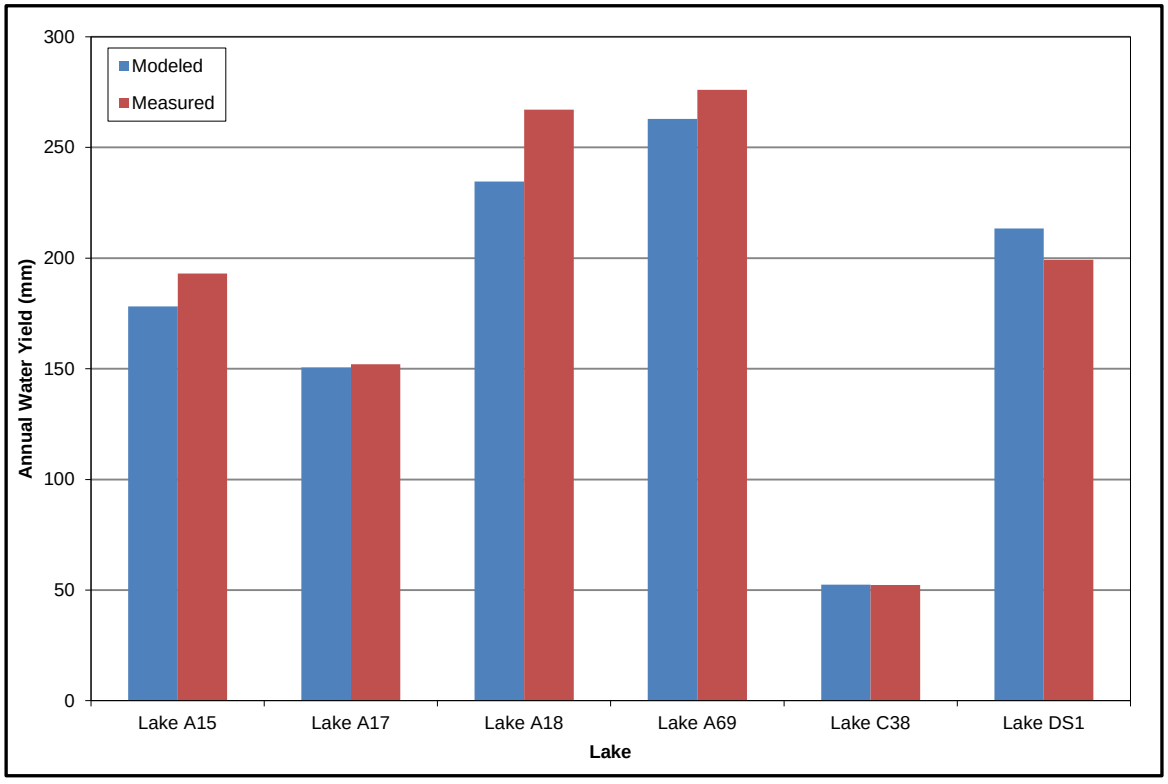

Figure C-23: Comparison of Modeled and Measured Water Yields in 2015

As a global, employee-owned organisation with over 50 years of experience, Golder Associates is driven by our purpose to engineer earth's development while preserving earth's integrity. We deliver solutions that help our clients achieve their sustainable development goals by providing a wide range of independent consulting, design and construction services in our specialist areas of earth, environment and energy.

For more information, visit golder.com

Africa	+ 27 11 254 4800
Asia	+ 86 21 6258 5522
Australasia	+ 61 3 8862 3500
Europe	+ 44 1628 851851
North America	+ 1 800 275 3281
South America	+ 56 2 2616 2000

solutions@golder.com
www.golder.com

Golder Associates Ltd.
16820 107 Avenue
Edmonton, Alberta, T5P 4C3
Canada
T: +1 (780) 483 3499

Golder Associates